

Forecasting using alternative measures of model-free option-implied volatility

Xingzhi Yao  | Marwan Izzeldin

Department of Economics, Lancaster
University Management School,
Lancaster, UK

Correspondence

Xingzhi Yao, Department of Economics,
Lancaster University Management School,
Lancaster, LA1 4YX, UK.
Email: x.yao@lancaster.ac.uk

Funding information

Economic and Social Research Council,
Grant number: ES/J500094/1

This paper evaluates the performance of various measures of model-free implied volatility in predicting returns and realized volatility. The critical role of the out-of-the money call options is highlighted through an investigation of the relevance of different components of the model-free implied volatility. The Monte Carlo simulations show that: first, volatility forecasting performance of various measures can be enhanced by employing an interpolation-extrapolation technique; second, for most measures considered, gains in their predictive power for future returns can be obtained by implementing an interpolation procedure. An empirical application using SPX options recorded from 2003 to 2013 further illustrates these claims.

JEL CLASSIFICATION

C63, G13, G17

1 | INTRODUCTION

In an efficient market, the option price embodies all available useful information about future movements of the underlying asset. Hence, traders and hedge fund managers are primarily interested in option-implied volatility when making financial decisions. As a natural forecast of return variation over the remaining life of the relevant option, option-implied volatility has been frequently used in forecasting future volatility, see Poon and Granger (2003) for an extensive review of the studies on this topic. As opposed to the Black–Scholes (BS) implied volatility, model-free option-implied volatilities have gained substantial popularity because, relying upon no particular parametric model, they avoid potential mis-specification problems. See, for example, Britten-Jones and Neuberger (2000), Carr and Wu (2006), and Taylor, Yadav, and Zhang (2010).

One of the most widely adopted measures of model-free option-implied volatility is the *VIX* volatility index, disseminated by the Chicago Board of Options Exchange (CBOE). The *VIX* provides a measure of the expected value of the S&P 500 return variation under the risk-neutral measure and is designed to closely mimic the model-free implied volatility (*MFIV*). Derived by Britten-Jones and Neuberger (2000), the *MFIV* is defined as an integral of cross-section of out-of-the money (OTM) European style put and call options over an infinite range of strikes for the given maturity. Jiang and Tian (2005) show that the *MFIV* is a more efficient forecast for future realized volatility than the BS implied volatility and the historical realized volatility. However, Andersen and Bondarenko (2007) argue that the *MFIV* and *VIX* are biased forecasts of future volatility since they contain non-trivial and time-varying risk premiums. As a more important part of their empirical study, Andersen and Bondarenko (2007) investigate the properties of the corridor implied volatility index (*CX*), which is obtained from the *MFIV* by truncating the integration domain between two barriers. Being less sensitive to variation in the market variance risk premium, the *CX* with the narrowest corridor width is found to dominate other implied volatility measures in the work of Andersen and Bondarenko (2007). Another advantage of the *CX* is that it is constructed only over intervals of the risk-neutral density (RND) where price quotes are directly observable. By contrast, the computation

requirements for deriving the *MFIV* are not satisfied by the existing data as options are traded only over a finite range of strikes. Andersen, Bondarenko, and Gonzalez-Perez (2015) further improve the construction of the *CX* by adopting the concept of an invariant coverage across time, which ensures that the *CX* is coherent in the time series dimension. As compared with the *VIX*, which is based upon strongly time-varying coverage of the tails of the RND, the *CX* uses a consistent range of strikes, which serves as a more accurate volatility indicator over time.

In addition to the use of implied volatilities in forecasting future volatility, prior studies also indicate that the *VIX* may carry some predictive power for future returns on stock market indices. For example, Giot (2005) finds that future returns are always positive (negative) for very high (low) levels of the *VIX*. This accords with the work of Guo and Whitelaw (2006) who provide evidence for the positive relationship between market returns and implied volatilities. The positive relationship between the *VIX* and future returns is also documented in Banerjee, Doran, and Peterson (2007) who suggest that both levels and innovations of the *VIX* are significantly related to future returns. That finding is indicative of a negative volatility risk premium, which is consistent with Ang, Hodrick, Xing, and Zhang (2006) where stocks with high past sensitivities to the innovation in the *VIX* display on average future decreasing returns. The evidence that the *VIX* is a priced risk factor in the time series of returns helps to explain why the *VIX* may exhibit predictive power for future returns. Although a substantial empirical literature is devoted to the investigation of risk-return relations (see, e.g., the discussion in Rossi & Timmermann (2010), and the many references therein), most rely on the *VIX* as a directly observable proxy for risk. Other measures of model-free option-implied volatility are rarely considered.

Despite the increasing popularity of the *VIX*, measurement errors in its construction have been noted by Jiang and Tian (2005). The common problem inherent in the computation of the *VIX* as well as other measures of model-free implied volatility is that only a discrete set of strikes is actually traded in the market and that very low and high strikes are usually absent. To account for measurement errors induced by the limited number of strikes, Jiang and Tian (2005) apply the cubic spline method to interpolate between existing strikes and exploit a flat extrapolation scheme to infer option prices beyond the truncation point. Andersen and Bondarenko (2007) address the issue induced by the discrete set of strikes via the positive convolution approximation method proposed by Bondarenko (2003). Although interpolation and extrapolation techniques are widely accepted, it remains unclear how such techniques affect the performance of implied volatilities in predicting future returns and realized volatility. In addition, there appears to be no consensus on the roles played by the OTM call and put options in the forecast of future volatility and returns. Jackwerth (2000), Jones (2006), and Bates (2008) suggest that the OTM put options may be irrelevant to known risk factors affecting stock returns. Using a cubic spline interpolation and flat extrapolation methods, Dotsis and Vlastakis (2016) also find that the OTM put options, especially deep OTM puts, do not contain important information with respect to equity volatility risk. They also show that the OTM call options subsume all useful information embedded in the OTM puts for forecasting future realized volatility. However, Andersen, Fusari, and Todorov (2015) show that the left tail risk, driving a substantial part of the OTM put option dynamics, exhibits strong predictive power for future excess market returns over long horizons.

Against this background, this study examines the performance of various model-free option-implied volatilities in predicting future returns and volatility and contribute to the existing literature in the following ways. First, this paper is among the first to provide simulation evidence to justify the use of the interpolation/extrapolation procedure for better forecasting performance of implied volatilities. The usefulness of this procedure is verified in both the simulation and empirical studies. The adoption of a stochastic volatility model with both jumps and volatility risk premium in the present study mimics more closely the observed data dynamics. This can be seen as an extension of the work of Zhang, Taylor, and Wang (2013) where a simple square-root model of Cox, Ingersoll, and Ross (1985) is employed to investigate the number of options upon the information content of the *MFIV* in an in-sample analysis. Distinct from Zhang et al. (2013), this paper conducts comprehensive out-of-sample (OOS) volatility forecasts made by different implied volatility measures including the *MFIV*.

Second, to ascertain the relevance of the OTM call and put options, this paper considers implied volatility measures constructed entirely from the cross-section of OTM put (call) options and measures which discard the deep OTM put (call) options. This is achieved by splitting the *MFIV* into different components with the use of different intervals of the cross-section of OTM put and call option prices. Similar constructions of implied volatilities are conducted in Dotsis and Vlastakis (2016) who examine the price of volatility risk in the cross-section of stock returns. With a different focus from that of Dotsis and Vlastakis (2016), the present paper compares the fraction of the time-series variation in future returns that are explained by various measures of implied volatility. Return predictability provided by implied volatilities is investigated in the pre- and post-crisis periods, respectively. The impact of the recent financial crisis is accounted for since the crisis represents an informative period during which uncertainty and risk aversion may have been more evident than the non-crisis period, see Hilal, Poon, and Tawn (2011) and Bates (2012).

A preview of the main findings of this study is as follows. Simulation results show that, with a wider range of strikes upon which model-free option-implied volatilities are based, the OOS volatility forecast becomes more accurate while returns tend to be less predictable. In addition, a finer partition of strikes usually leads to greater predictive power of implied volatilities for future returns. These findings warrant the application of an interpolation and extrapolation scheme in the practice of volatility forecast and an interpolation method only in return predictions. In the empirical study using SPX options from 2003 to 2013, the aforementioned procedure, that is, interpolation/extrapolation methods, significantly improves the performance of different measures of implied volatility considered in the OOS volatility forecast and gives rise to higher return predictability for most measures in the post-crisis period. With the use of this procedure, the OTM SPX call options substantially dominate the OTM put options with regard to their forecasting performance. The empirical findings outlined above are in accordance with the simulation evidence. Furthermore, when measures of implied volatility are derived from the listed options only, the superiority of the OTM SPX put options over the OTM call options is noted in volatility forecast and post-crisis return predictions.

The rest of this paper is organized as follows. Section 2 provides the construction of various model-free option-implied volatility measures and realized volatility adopted in this study. Section 3 outlines the techniques adopted to address measurement errors in the construction of various implied volatilities. Section 4 presents the design and settings of the Monte Carlo study along with the results. Section 5 describes the data and section 6 reports the empirical results. Conclusion is provided in section 7.

2 | CONSTRUCTION OF VOLATILITY MEASURES

This section provides an outline of the construction of various measures of volatility. Section 2.1 gives an introduction of the *MFIV* and its components derived from OTM calls and OTM puts, respectively. The *VIX* index is then reviewed as a close approximation of the *MFIV*. Section 2.2 discusses the computation of model-free corridor implied volatilities where three different segments of the cross-section of OTM put and call option prices are adopted. Finally, in section 2.3, the high-frequency realized volatility is defined, which is used to obtain an accurate measure of the ex-post return variation of the underlying asset.

2.1 | Model-free implied volatility and VIX

The concept of the *MFIV* is derived by Britten-Jones and Neuberger (2000). Its computation for a given maturity involves market prices for a continuum of European-style options with strikes from zero to infinity, which takes the form

$$MFIV = \sqrt{\frac{2}{\tau} e^{r\tau} \left[\int_0^F \frac{P(\tau, K)}{K^2} dK + \int_F^\infty \frac{C(\tau, K)}{K^2} dK \right]} \quad (1)$$

where r is the annualized risk-free interest rate as measured by the corresponding U.S. Treasury bill rate, τ is time-to-maturity measured in annual units, F is the forward price for transaction at maturity τ , $P(\tau, K)$ and $C(\tau, K)$ are the mid-quotes for European put and call options with strike price K and maturity τ . By construction, only OTM options (call if $K > F$ and put otherwise) are taken into account. Motivated by Dotsis and Vlastakis (2016), the *MFIV* can be further divided into two components; that is, that from the OTM call options (*VC*) and that from the OTM put options (*VP*), which are given by

$$VC = \sqrt{\frac{2}{\tau} e^{r\tau} \int_F^\infty \frac{C(\tau, K)}{K^2} dK} \quad (2)$$

and

$$VP = \sqrt{\frac{2}{\tau} e^{r\tau} \int_0^F \frac{P(\tau, K)}{K^2} dK} \quad (3)$$

where $MFIV^2 = VC^2 + VP^2$.

The *VIX* index is based on the idea of fair value of future volatility developed by Demeterfi, Derman, Kamal, and Zou (1999), which is conceptually equivalent to the *MFIV* in equation (1) as shown by Jiang and Tian (2007). The general formula for computation of the *VIX* index is given by

$$VIX = \sqrt{\frac{2}{\tau} \sum_i \frac{\Delta K_i}{K_i^2} e^{r\tau} Q(\tau, K_i) - \frac{1}{\tau} \left(\frac{F}{K_0} - 1 \right)^2} \quad (4)$$

where $\tau = 30/365$ is the option maturity, K_i is the strike price of the i th OTM option in the calculation,¹ K_0 is the first strike price below the forward index level F ($K_0 \leq F$), $Q(\tau, K_i)$ is the midpoint of the latest available bid and ask prices of the OTM option at strike K_i , and ΔK_i stands for the strike price interval as $\Delta K_i = (K_{i+1} - K_{i-1})/2$.

2.2 | Corridor implied volatility

The corridor implied volatility index (CX) is initially analyzed in the empirical work of Andersen and Bondarenko (2007). Unlike the $MFIV$, which requires the availability of options with strikes from zero to infinity, the CX only captures volatility over a certain segment of the underlying RND. For a fixed coverage $[B_L, B_H]$, $0 \leq B_L \leq B_H \leq \infty$, the CX is computed as

$$CX = \sqrt{\frac{2e^{r\tau}}{\tau} \int_{B_L}^{B_H} \frac{M(K)}{K^2} dK} \quad (5)$$

where the time to maturity $\tau = 30$ days and $M(K)$ stands for the minimum of the put and call prices at current time such as

$$M(K) = \min(P(\tau, K), C(\tau, K))$$

In order to ensure an invariant portion of the strike range considered in the CX across time, Andersen, Bondarenko, and Gonzalez-Perez (2015) propose the ratio $R(K)$ to determine the integration barriers of the CX in equation (5) using directly observable prices of OTM call and put options only,

$$R(K) = \frac{P(\tau, K)}{P(\tau, K) + C(\tau, K)} \quad (6)$$

For given lower and upper percentiles $p, q \in (0, 1)$, $B_L = K_p = R^{-1}(p)$, and $B_H = K_{1-q} = R^{-1}(1 - q)$. In the subsequent simulation and empirical studies, three measures of the CX computed from equation (5) are used where $[B_L, B_H]$ takes the values $[R^{-1}(0.25), R^{-1}(0.75)]$, $[R^{-1}(0), R^{-1}(0.75)]$, and $[R^{-1}(0.25), R^{-1}(1)]$. These implied volatilities are respectively represented by $CXNT$, $CXLT$, and $CXRT$. The definitions of implied volatilities considered in this paper are listed in Table 1. All the measures are computed from options across two nearest maturities (less than 30 days and greater than 30 days) and the 30-day implied volatilities is computed by interpolating between the two separate maturities.

2.3 | Realized volatility

In addition to implied volatilities, this study employs monthly realized volatility and historical volatility. A simple realized variance estimator proposed by Barndorff-Nielsen and Shephard (2002) is employed, which is equal to the sum of intraday squared returns

¹The forward price is calculated from at-the-money options according to put-call parity, $F = K_* + e^{r\tau} [C(K_*, \tau) - P(K_*, \tau)]$ and K_* is determined as the strike price for which the difference between the call and put prices is minimal. It is worth noting that, at the boundaries of strike prices, ΔK_i is adjusted as the difference between the two highest (or lowest) strike prices. In addition, at the strike price K_0 , the option price $Q_i(\tau, K_i)$ is modified to be the average of call and put prices. The CBOE computes the VIX from an interpolation of two volatility indices with respect to two different maturities: τ'_l and τ''_l . The VIX index is finally obtained by taking a weighted average of these two VIX measures based on τ'_l and τ''_l

$$VIX = 100 \times \sqrt{w_1 (VIX_{\tau'_l}^2) \tau'_l + w_2 (VIX_{\tau''_l}^2) \tau''_l} \times \frac{365}{30} \quad (19)$$

where $w_1 = \frac{\tau''_l - \tau}{\tau''_l - \tau'_l}$ and $w_2 = \frac{\tau - \tau'_l}{\tau''_l - \tau'_l}$ so that $w_1 + w_2 = 1$.

TABLE 1 This table lists the definitions of various measures of model-free implied volatility adopted in this study

Measures	Definition
VIX_{Theo}	The theoretical VIX index under the stochastic volatility-jump model, see more details in Duan and Yeh (2010).
VIX	The VIX index published by the CBOE, see equation (4) in main text.
RX	The replicated VIX index, an equivalent of the VIX using the SPX options from the Optionmetrics data set.
MFIV	The model-free implied volatility computed from the full cross-section of OTM put and call options, see equation (1) in main text. In the empirical study, the MFIV is computed using equation (4) while ignoring the cutoff rule by the CBOE.
CXNT	The corridor implied volatility computed from the cross-section of OTM put and call options that truncate the left and right tails of the underlying risk-neutral density by 25%.
CXLT	The corridor implied volatility computed from the cross-section of OTM put and call options that truncate the right tail of the underlying risk-neutral density by 25%.
CXRT	The corridor implied volatility computed from the cross-section of OTM put and call options that truncate the left tail of the underlying risk-neutral density by 25%.
VC	The model-free implied volatility computed from the full cross-section of OTM call options, see equation (2) in main text.
VP	The model-free implied volatility computed from the full cross-section of OTM put options, see equation (3) in main text.
CP-	Measures constructed by options with the use of an interpolation and extrapolation scheme.
C-	Measures constructed by options with the use of an interpolation method.

$$rv_t = \sum_{j=1}^M r_{t,j}^2 \quad (7)$$

where $r_{t,j}$ stands for intraday returns within each 5-min interval. The realized variance is then calculated over a period of 1 month in order to match the maturities of the corresponding implied volatilities

$$RV_t = \frac{1}{22} \sum_{i=1}^{22} rv_{t+i} \quad (8)$$

The measure RV_t is recorded daily but contains monthly (future) variance. The substantial serial correlation induced by the construction of RV_t in equation (8) will be accounted for in the subsequent analysis. Furthermore, the realized variance on the latest trading day, rv_{t-1} is used as a proxy for historical variance, which may contain useful information for future return variation.

3 | ERROR ADJUSTMENT MECHANISMS

As introduced in section 2, the *MFIV* is computed as an integral of option prices over an infinite range of strikes; and all the measures of implied volatility that are considered require numerical integration using the trapezoidal rule. However, only a limited number of strikes are actually traded in the market, which may result in inaccuracies in the computation of the option-implied volatilities, so further affecting their performance in predicting future volatility and returns. Specifically, very low and high strikes are usually not available in practice, which leads to the so-called truncation errors; and the set of discrete strikes can be rather sparse, which gives rise to the discretization errors. For more details,² see Jiang and Tian (2005). To account for the measurement errors discussed above, the use of an interpolation and extrapolation scheme is essential. The interpolation of option prices within the boundary of actual strikes is relatively straightforward, which can be carried by fitting a natural cubic spline as in the work of Jiang and Tian (2005). The major challenge is how to extrapolate option prices toward the tails of the RND with precision. The following section provides an introduction of the extrapolation procedure adopted in the present paper.

In line with Andersen and Bondarenko (2007), this paper estimates the RND using a nonparametric approach, the so-called positive convolution approximation (PCA) proposed by Bondarenko (2003) and then extracts prices beyond

²Other measurement errors noted by Jiang and Tian (2007) are widely regarded as negligible and therefore are unlikely to have any material impact on the forecasting performance of implied volatilities.

the truncation point from the estimated RND.³ The PCA method for estimating the RND offers several benefits: (i) it guarantees no-arbitrage density estimates; (ii) it avoids overfitting while allowing for small samples; (iii) it involves simple computation algorithm only; and (iv) it is insensitive to the data generating process. The main idea of the PCA is to construct a set of admissible densities containing functions which can be expressed as a convolution of a fixed positive kernel and another density. The optimal density is that obtained from the admissible densities which generates the best fit to the listed option prices. The sub-section below briefly describes the RND estimation using the PCA approach.

The relationship between the RND and call/put options can be expressed as

$$h_0(S_\tau) = \frac{1}{e^{\int_0^\tau r_s ds}} \frac{\partial^2 C(\tau, K)}{\partial K^2} \bigg|_{K=S_\tau} = \frac{1}{e^{\int_0^\tau r_s ds}} \frac{\partial^2 P(\tau, K)}{\partial K^2} \bigg|_{K=S_\tau} \quad (9)$$

where S_τ represents the value of an underlying asset on trading date τ and r_s is the risk-free rate. For simplicity, it is assumed that the asset pays no dividends and $r_s = 0$ and thus $e^{\int_0^\tau r_s ds} = 1$. In the PCA approach, the first step is to construct the approximating set W_h representing all admissible or candidate densities, from which the optimal density is selected. Let L^d denote the set of all probability densities, that is, nonnegative functions that integrate to one. For a basis density $\phi(K) \in L^d$, a new density $\phi_m(K) := \frac{1}{m} \phi\left(\frac{K}{m}\right)$ can be obtained by smoothing $\phi(K)$ with the bandwidth parameter m . Once $\phi_m(K)$ is fixed, the approximating set $W_m = W_{\phi_m}$ is given by

$$W_m := \{g \in L^d \mid g = \phi_m \times \mu, \text{ for } \mu \in L^d\} \quad (10)$$

which contains functions g , expressed as a convolution of ϕ_m with positive functions μ . Although the space L^d accommodates very general shapes of densities, W_m is made up of only smooth and well-behaved densities. If functions h (the true RND) and g are both integrable, the following equation holds.

$$h \times g := \int_{-\infty}^{\infty} h(K-y)g(y)dy \quad (11)$$

An estimator of the RND is the function of $\hat{h}(K) \in W_m$ which provides the best fit to a certain cross-section of options $\{P_i\}$, that is, it achieves the objective function as follows

$$\underset{\hat{h} \in W_m}{\text{Minimize}} \sum_{i=1}^n \left(P_i - D^{-2} \hat{h}(K_i) \right)^2 \quad (12)$$

where $D^{-2}g(K)$ represents the second integral of $g(K)$ such as

$$D^{-2}g(K) := \int_{-\infty}^K \left(\int_{-\infty}^y g(z)dz \right) dy \quad (13)$$

The optimization problem in equation (12) can be solved numerically by discretizing the admissible set W_m as follows

$$\underset{\hat{h} \in W_m^{\Delta z}([v,w])}{\text{Minimize}} \sum_{i=1}^n \left(P_i - D^{-2} \hat{h}(K_i) \right)^2 \quad (14)$$

with $\Delta z = 0.5m$, where $[v,w]$ is a large but finite interval on which the underlying density h is approximated and Δz is the grid step. Further details on the construction of the PCA estimator can be found in Bondarenko (2003). Once the

³Different ways of interpolation and extrapolation were attempted in this study. For example, the clamped cubic spline interpolation and the smoothing spline delivered results similar to those based on the natural cubic spline technique. In addition, attempts were made to extend the tails of the RND using the flat-line extrapolation and to approximate the tails of the RND following a generalized extreme value distribution. These methods are dominated by the use of the PCA approach as introduced in the main text.

estimated RND is obtained, option prices can be inferred for a continuum of strikes through the relationship in equation (9).

4 | MONTE CARLO SIMULATION

This section presents a Monte Carlo simulation study where different numbers of option prices are considered as the strike range and increment vary. The aim of this experiment is (i) to ascertain the impact of discrete strike prices on the performance of various implied volatility measures in forecasting future volatility and returns and (ii) to provide guidance for the use of interpolation and extrapolation technique in forecasting.

4.1 | Simulation design

The simulation exercise conducted in the present paper is motivated by Zhang et al. (2013) who examine the effect of the number of strikes on the information content of the *MFIV* using a simple model without jumps and volatility risk premium. In a departure from Zhang et al. (2013), this study concentrates on the OOS volatility forecasting performance of implied volatilities and the predictive power of implied volatilities for future returns. A jump-diffusion model adopted by Duan and Yeh (2010) is used to simulate the asset price and the latent stochastic volatility by

$$\begin{aligned} d \ln S_t &= \left[r - q + \delta_s V_t - \frac{V_t}{2} \right] dt + \sqrt{V_t} dW_t + J_t dN_t - \lambda \mu_J dt \\ dV_t &= \kappa(\theta - V_t)dt + vV_t^\gamma dB_t \end{aligned} \quad (15)$$

where W_t and B_t are correlated Wiener processes, having correlation coefficient equal to ρ ; N_t denotes a Poisson process with intensity λ , which is independent of W_t and B_t ; J_t is an independent normal random variable with mean μ_J and standard deviation σ_J . The price, S_t , and volatility, V_t , processes are dependent through the correlated diffusive terms — W_t and B_t . The other parameters, r , q and δ_s are the risk-free rate, the dividend yield and the asset risk premium, respectively.⁴

Option valuation is implemented using the corresponding model under the risk-neutral probability measure given by

$$\begin{aligned} d \ln S_t &= \left[r - q - \frac{V_t}{2} + \lambda^* \left(\mu_J^* + 1 - e^{\mu_J^* + \sigma_J^2} \right) \right] dt + \sqrt{V_t} dW_t^* + J_t^* dN_t^* - \lambda^* \mu_J^* dt \\ dV_t &= (\kappa\theta - \kappa^* V_t)dt + vV_t^\gamma dB_t^* \end{aligned} \quad (16)$$

where $\kappa^* = \kappa + \delta_V$ and $B_t^* = B_t + \delta_V/v \int_0^t V_s^{1-\gamma} ds$ with δ_V being the volatility risk premium. Again, W_t^* and B_t^* are the Wiener processes correlated with the coefficient ρ ; N_t^* is a Poisson process with intensity λ^* independent of W_t^* and B_t^* ; the independent normal random variable J_t^* has a new mean μ_J^* but an unchanged standard deviation σ_J . The empirical martingales simulation method⁵ developed by Duan and Simonato (1998) is used to compute option prices, given that there is no closed-form option pricing formula for equation (16). In addition, the theoretical *VIX* index, represented by VIX_{Theo} , is computed by following the work of Duan and Yeh (2010).

This study assumes 1 year has 252 trading days and that 1 day consists of 6.5 hr of open trading, as is the case on the NYSE and NASDAQ. A sparse sampling at a frequency of once every 5 min is used in this simulation study and therefore 1 day can be divided up into 78 intraday intervals, that is, $\frac{6.5 \times 3600}{300} = 78$. A daily series is extracted by sampling once every 78 data points. The asset price and the latent stochastic volatility are simulated according to the Euler

⁴The mean of $J_t dN_t - \lambda \mu_J dt$ is zero due to the introduction of the term $\lambda \mu_J dt$, which serves to center the Poisson innovation.

⁵The simulation sample path is set to 1000. Put option prices are computed through put-call parity.

discretized version⁶ of equation (15). The simulation is simplified by assuming no dividends and a zero interest rate. The initial stock price and latent stochastic volatility⁷ are set respectively as 1000 and 0.08. The sample size of daily series is 2000. The parameter values are similar to those adopted by Duan and Yeh (2010).

κ	θ	λ	$\mu_J(\%)$	$\sigma_J(\%)$	v	ρ	γ	δ_s	κ^*	$\phi^*(\%)$	δ_V	$\delta_J(\%)$
2.500	0.080	55.000	0.300	0.500	1.400	-0.800	0.900	0.420	-13.000	0.035	-15.500	-0.059

Option prices are computed corresponding to two nearby maturities, 23 and 37 days. This experiment considers two fixed strike price increments ($\Delta K = 5$ and $\Delta K = 1$) and attempts with different moneyness ranges ($[0.8, 1.2]$, $[0.7, 1.3]$, and $[0.6, 1.4]$).

4.2 | Simulation results

Table 2 reports the summary statistics of various volatility measures. It is evident that the mean of the implied volatility estimates increases with the moneyness range. This accords with the work of Jiang and Tian (2007), where the truncation errors usually result in an underestimation of the true volatility. The mean of the *VIX*, *MFIV*, *CXNT*, *CXLT*, and *CXRT* decreases as the strike increment becomes smaller, which is consistent with the finding of overestimation of the underlying volatility induced by discretization errors in Jiang and Tian (2007). For all measures considered, the mean squared error⁸ (MSE) decreases with the strike range. Table 2 also shows that measures of implied volatility become more volatile with the range of strikes while they, except the *VC*, tend to appear less volatile as the partition of strikes is smaller.

To evaluate the OOS volatility forecasting performance of various option-implied volatilities, a univariate Mincer-Zarnowitz regression is adopted as follows

$$y_{t+1} = \alpha_j + \beta_j x_{j,t} + \mu_{j,t+1} \quad (17)$$

where y_{t+1} represents the realized volatility containing the information of month $t + 1$ and where $x_{j,t}$ indicates the volatility estimate j among all candidate estimates. To obtain OOS forecasts of the realized volatility measure, this study employs a rolling window of 1000 observations for the one-step-ahead forecasts. The daily realized volatility in equation (8) contains substantial induced serial correlation, which seriously affects the standard errors of the coefficient estimates. To overcome this problem, the Bartlett/Newey–West heteroskedasticity consistent covariance matrix estimator with 44 lags is used, see Andersen, Bollerslev, and Diebold (2007). Regressions are examined for both volatility and logarithms of volatility. The forecasts are evaluated by the MSE, which is robust to the presence of noise in the volatility proxy, see Patton (2011). The OOS R^2 of the Mincer-Zarnowitz regression is also taken into account, which corrects for bias by reflecting the variance but not the bias-squared component of the MSE.

Forecasting results⁹ are reported in Table 3. Clearly, the VIX_{theo} dominates all the other candidate measures in terms of the volatility forecasting performance.¹⁰ Forecasting performance increases with the strike range for all the measures, except that of the *CXNT* and *CXLT*. It is not surprising that the *CXNT* performs the same for different moneyness ranges since the options

⁶The asset price and volatility path will be discretized into constant-increment time steps of $\Delta t = \frac{1}{78 \times 252}$. The discretization for the price and volatility processes through Euler scheme is given by

$$S_{t+1} = S_t \exp[(r - q + \delta_s V_t - 0.5 V_t) \Delta t + \sqrt{V_t \Delta t} W_t + J_t N_t - \lambda \mu_J \Delta t]$$

$$V_{t+1} = V_t + (\kappa \theta - \kappa V_t) \Delta t + \rho v V_t^\gamma \sqrt{\Delta t} W_t + \sqrt{1 - \rho^2} v V_t^\gamma \sqrt{\Delta t} B_t$$

where J_t is i.i.d. $N(\mu_J, \sigma_J)$, N_t is Poiss($\lambda \Delta t$), W_t and B_t are two Brownian-motion processes, and ρ represents the instantaneous correlation between the return process and the volatility process. As introduced in the main text, $S_0 = 1000$ and $V_0 = 0.08$.

⁷This study also considers a low volatility setting by letting the initial latent stochastic volatility equal 0.02. Conclusions remain unchanged.

⁸This is defined as the time-series average of the squared differences between the certain volatility estimate and the theoretical *VIX* index, VIX_{theo} .

⁹Motivated by the study of Andersen, Bondarenko, and Gonzalez-Perez (2015), this study also attempts to construct the realized variance using the sum of a weighted average of the log and simple squared returns, represented by RV^w . Values of the MSE for the forecasts of RV^w remain virtually unchanged.

¹⁰In several situations, the $rv_t - 1$ outperforms option-implied volatility estimates, which seems to contradict the findings of Jiang and Tian (2005) and Andersen and Bondarenko (2007). The explanation is that this experiment considers the case of very high volatility, that is, $V_0 = 0.08$. When the initial latent stochastic volatility is set lower, the performance of daily lagged *RV* falls as compared with the other implied volatility measures.

TABLE 2 Simulation study: summary Statistics

			Mean	Std Dev	25%	50%	75%	MSE
VIX_{Theo}			39.1297	14.3567	29.4363	35.3602	43.8213	
RV			23.6841	9.4726	17.2824	21.5069	26.7618	
$\Delta K = 5$	N_K	Moneyness range						
VIX	86	[0.8, 1.2]	36.2688	11.3866	28.1721	33.8260	41.4539	29.1182
	128	[0.7, 1.3]	37.7167	12.9644	28.6248	34.6614	43.2231	16.8826
	167	[0.6, 1.4]	38.2435	13.8219	28.6925	34.8117	43.7395	14.2855
$MFIV$	86	[0.8, 1.2]	36.9711	11.3161	28.8961	34.5055	42.2275	25.6308
	128	[0.7, 1.3]	38.6101	13.0396	29.4648	35.5447	44.2569	14.7022
	167	[0.6, 1.4]	39.2324	13.9959	29.5486	35.7811	44.8681	13.1674
$CXNT$	86	[0.8, 1.2]	27.9266	10.2982	20.9701	25.4019	31.7878	150.4968
	128	[0.7, 1.3]	27.9266	10.2982	20.9701	25.4019	31.7878	150.4968
	167	[0.6, 1.4]	27.9266	10.2982	20.9701	25.4019	31.7878	150.4968
$CXLT$	86	[0.8, 1.2]	34.2586	10.9680	26.5616	31.8153	39.0299	47.3269
	128	[0.7, 1.3]	35.6924	12.3049	27.0270	32.7474	40.9577	30.1992
	167	[0.6, 1.4]	36.2805	13.1204	27.1798	32.9743	41.6377	24.6749
$CXRT$	86	[0.8, 1.2]	31.2108	10.6210	23.8673	28.6452	35.5908	84.5573
	128	[0.7, 1.3]	31.5717	11.1677	23.8923	28.7841	36.0049	74.6089
	167	[0.6, 1.4]	31.6768	11.4019	23.8933	28.8077	36.0561	71.2892
VC	86	[0.8, 1.2]	22.9491	7.2992	17.7665	21.2982	26.0928	316.1882
	128	[0.7, 1.3]	23.4417	8.0621	17.8222	21.4521	26.5423	289.5784
	167	[0.6, 1.4]	23.5835	8.3822	17.8222	21.4761	26.6604	280.8594
VP	86	[0.8, 1.2]	28.4255	8.5915	22.2635	26.6314	32.5155	161.1815
	128	[0.7, 1.3]	30.1422	10.2282	22.8413	27.8142	34.7325	113.4245
	167	[0.6, 1.4]	30.8299	11.1983	23.0182	28.0057	35.4366	95.2843
$\Delta K = 1$								
VIX	422	[0.8, 1.2]	36.1206	11.2236	28.1317	33.7444	41.3216	31.0087
	629	[0.7, 1.3]	37.6563	12.8712	28.6170	34.6308	43.1692	17.3348
	1239	[0.6, 1.4]	38.2166	13.7685	28.6902	34.8077	43.7299	14.3939
$MFIV$	422	[0.8, 1.2]	36.8572	11.1951	28.8665	34.4344	42.1000	26.8896
	629	[0.7, 1.3]	38.5635	12.9668	29.4599	35.5384	44.2100	14.9503
	1239	[0.6, 1.4]	39.2117	13.9525	29.5504	35.7789	44.8443	13.1920
$CXNT$	422	[0.8, 1.2]	27.6792	10.2485	20.7987	25.1750	31.5773	156.4750
	629	[0.7, 1.3]	27.6792	10.2485	20.7987	25.1750	31.5773	156.4750
	1239	[0.6, 1.4]	27.6792	10.2485	20.7987	25.1750	31.5773	156.4750
$CXLT$	422	[0.8, 1.2]	34.0638	10.8394	26.4723	31.6732	38.8431	50.1150
	629	[0.7, 1.3]	35.5644	12.2193	26.9314	32.6610	40.8070	31.4616
	1239	[0.6, 1.4]	36.1791	13.0634	27.0938	32.8640	41.5633	25.4219
$CXRT$	422	[0.8, 1.2]	31.0706	10.5707	23.7608	28.5266	35.5119	87.1688
	629	[0.7, 1.3]	31.4414	11.1297	23.8061	28.6810	35.9053	76.8183
	1239	[0.6, 1.4]	31.5491	11.3691	23.8061	28.6948	35.9247	73.3751
VC	422	[0.8, 1.2]	23.2036	7.3257	18.0626	21.5130	26.4031	307.5802
	629	[0.7, 1.3]	23.7030	8.0965	18.0836	21.6831	26.9452	280.9600
	1239	[0.6, 1.4]	23.8465	8.4200	18.0880	21.6981	27.0022	272.2445
VP	422	[0.8, 1.2]	28.5067	8.5052	22.4153	26.7591	32.5390	160.2375

(Continues)

TABLE 2 (Continued)

		Mean	Std Dev	25%	50%	75%	MSE
629	[0.7, 1.3]	30.2902	10.1843	23.0286	28.0615	34.8485	110.9583
1239	[0.6, 1.4]	31.0050	11.1826	23.1910	28.3104	35.7387	92.3282

This table reports the mean, standard deviation, lower quartile (25%), median (50%), and upper quartile (75%) of daily annualized volatility estimates over 2000 days. All the values are percentages. The mean squared estimation error, MSE, is the average of the squared differences between the volatility estimates and the theoretical VIX_{theo} . The strike price increment is denoted by ΔK and N_K refers to the number of available options on each estimation day.

within the barriers $B_L = K_{0.25}$ and $B_H = K_{0.75}$ are not affected by the variation in the strike range. The worse performance of the *CXLT* with a wider range of strikes may be attributed to the poor forecasting power of the deep OTM put options for future volatility. In addition, Table 3 shows that the strike increment ΔK tends to have a negative impact on the volatility forecasting power of the *VIX*, *MFIV*, *CXNT*, *CXLT*, and *CXRT* but exerts a positive impact on that of the *VC* and *VP*. Overall, the effect of the strike range on the forecasting performance is considerable and that of the strike increment is negligible. The use of different loss functions, that is, MSE and OOS R^2 , gives the identical conclusion in terms of the role of the strike range and increment in the forecasting practice as well as the ranking of forecast performance among implied volatility candidates. These findings motivate the application of an extrapolation procedure to extend the tails of the RND in an attempt to improve the volatility forecast accuracy. On the other hand, an interpolation method is considered necessary since the number of listed options may be rather small in practice. The lack of observed options may lead to inaccuracies in the estimation of the RND using the PCA method and thus result in failure in inferring the options beyond the truncation points. Moreover, the critical role of the OTM call options is noted in Table 3 where the *VC* serves as the top forecaster and the *CXRT* substantially outperforms the *CXLT*.

The next step is to apply the natural cubic spline to interpolate between available strikes and to implement the PCA method in order to obtain the option values beyond the range of listed strikes. The corresponding measures computed by options with the use of such procedure are prefixed by *CP*-. To examine the performance of the *CP*-measures in the forecasting practice for future volatility, this study focuses on the case of $\Delta K = 5$ and moneyness range = [0.8, 1.2] only. Specifically, a step of one unit of the index is used to numerically compute the integral in the interpolation procedure and four standard deviations from forward prices are adopted as an integration range.¹¹ The interval of strikes that are needed to extrapolate is $([F_0 - 4SD, K_{\min}] \text{ and } [K_{\max}, F_0 + 4SD])$ where $K_{\min}(K_{\max})$ represents the minimum (maximum) listed strike price in the market. Table 4 reports the volatility forecast performance, measured by both the MSE and OOS R^2 , of various implied volatility measures and their corresponding *CP*-measures. The values in parentheses below the MSE are the mean difference of squared forecasting errors between the original implied volatility measure and its corresponding *CP*-measure. Numbers in bold indicate statistically significant differences at 5% by the Diebold–Mariano test. Columns 1–4 show that the *CP-MFIV*, *CP-CXRT*, *CP-VC*, and *CP-VP* achieve significant gains in the forecasting performance for future volatility and that the ranking of forecasting power of the *CP*-measures remains unchanged from that of the original measures. Columns 5–8 present values of the OOS R^2 where the percentage changes of the R^2 are represented by the numbers in parentheses and where the gains of the *CP*-measures are indicated in bold. With the single exception of *CXNT*, the use of the interpolation and extrapolation method brings higher OOS R^2 for all the measures considered.

Another important application of the implied volatility is to predict future market returns. As in the work of Banerjee et al. (2007), the 30- and 60-day future returns are regressed on daily levels¹² of the implied variance estimates as follows

$$\frac{1}{h} \sum_{j=1}^h r_{t+(j-1), t+j} = \alpha_1 + \beta_1 v_t + u_{t, t+h} \quad (18)$$

where v_t indicates various measures of implied variance levels. To account for residual correlation caused by overlapping returns, this study considers the Newey–West standard errors. The adjusted R^2 is employed to indicate the degree of return predictability; the values are reported in Table 5. First, results indicate that the return predictions by implied volatility measures

¹¹The choice of the truncation point is motivated by the finding of Jiang and Tian (2005) who show that the truncation errors are virtually zero beyond 3.5SD from F_0 .

¹²As a robustness check, the analysis of return predictions is also conducted by regressing future returns on the innovations of the implied variances, motivated by the work of Banerjee et al. (2007). Conclusions remain unchanged.

TABLE 3 Simulation study: out-of-sample forecast losses

			MSE		Ranking		Out-of-sample R^2 (%)		Ranking	
			Volatility	Log volatility	Volatility	Log volatility	Volatility	Log volatility	Volatility	Log volatility
VIX_{Theo}			0.0387	0.0190			74.5090	76.8332		
rv_{t-1}			0.0558	0.0287			63.2640	65.1061		
$\Delta K = 5$	N_K	Moneyness Range								
VIX	86	[0.8, 1.2]	0.0568	0.0269	5	5	62.6171	67.2937	5	5
	128	[0.7, 1.3]	0.0553	0.0267			63.5527	67.5413		
	167	[0.6, 1.4]	0.0544	0.0265			64.2093	67.7660		
MFIV	86	[0.8, 1.2]	0.0564	0.0266	4	4	62.8468	67.6101	4	4
	128	[0.7, 1.3]	0.0551	0.0265			63.7494	67.7624		
	167	[0.6, 1.4]	0.0541	0.0264			64.3901	67.9136		
CXNT	86	[0.8, 1.2]	0.0519	0.0258	3	3	65.8194	68.6326	3	3
	128	[0.7, 1.3]	0.0519	0.0258			65.8194	68.6326		
	167	[0.6, 1.4]	0.0519	0.0258			65.8194	68.6326		
CXLT	86	[0.8, 1.2]	0.0577	0.0280	6	6	62.0262	65.9059	6	6
	128	[0.7, 1.3]	0.0582	0.0283			61.6691	65.5402		
	167	[0.6, 1.4]	0.0578	0.0283			61.9562	65.5705		
CXRT	86	[0.8, 1.2]	0.0504	0.0244	2	2	66.8396	70.3366	2	2
	128	[0.7, 1.3]	0.0489	0.0239			67.7939	70.9327		
	167	[0.6, 1.4]	0.0483	0.0238			68.1703	71.0847		
VC	86	[0.8, 1.2]	0.0496	0.0231	1	1	67.3493	71.8709	1	1
	128	[0.7, 1.3]	0.0467	0.0224			69.2267	72.6933		
	167	[0.6, 1.4]	0.0457	0.0223			69.9102	72.8904		
VP	86	[0.8, 1.2]	0.0662	0.0311	7	7	56.3911	62.1576	7	7
	128	[0.7, 1.3]	0.0651	0.0310			57.1374	62.2606		
	167	[0.6, 1.4]	0.0635	0.0307			58.1738	62.6052		
$\Delta K = 1$										
VIX	422	[0.8, 1.2]	0.0574	0.0270	5	5	62.1791	67.1571	5	5
	629	[0.7, 1.3]	0.0556	0.0267			63.3723	67.4821		
	1239	[0.6, 1.4]	0.0545	0.0265			64.1190	67.7361		
MFIV	422	[0.8, 1.2]	0.0569	0.0267	4	4	62.5251	67.5176	4	4
	629	[0.7, 1.3]	0.0553	0.0265			63.6167	67.7243		
	1239	[0.6, 1.4]	0.0542	0.0264			64.3310	67.9012		
CXNT	422	[0.8, 1.2]	0.0522	0.0259	3	3	65.6335	68.4597	3	3
	629	[0.7, 1.3]	0.0522	0.0259			65.6335	68.4597		
	1239	[0.6, 1.4]	0.0522	0.0259			65.6335	68.4597		
CXLT	422	[0.8, 1.2]	0.0582	0.0281	6	6	61.6776	65.7394	6	6
	629	[0.7, 1.3]	0.0586	0.0284			61.4355	65.4086		
	1239	[0.6, 1.4]	0.0580	0.0284			61.8023	65.4760		
CXRT	422	[0.8, 1.2]	0.0505	0.0244	2	2	66.7138	70.2520	2	2
	629	[0.7, 1.3]	0.0490	0.0239			67.7127	70.8682		
	1239	[0.6, 1.4]	0.0484	0.0238			68.1058	71.0259		
VC	422	[0.8, 1.2]	0.0487	0.0227	1	1	67.9035	72.3489	1	1

(Continues)

TABLE 3 (Continued)

			MSE		Ranking		Out-of-sample R^2 (%)		Ranking	
			Volatility	Log volatility	Volatility	Log volatility	Volatility	Log volatility	Volatility	Log volatility
VP	629	[0.7, 1.3]	0.0460	0.0221			69.7165	73.1407		
	1239	[0.6, 1.4]	0.0450	0.0219			70.3702	73.3265		
	422	[0.8, 1.2]	0.0664	0.0310	7	7	56.2748	62.3124	7	7
	629	[0.7, 1.3]	0.0649	0.0308			57.2576	62.4827		
	1239	[0.6, 1.4]	0.0632	0.0305			58.3920	62.8674		

This table reports the ratio of the losses (MSE and R^2) for different predictive regressions for future monthly realized volatility and logarithm of volatility, respectively. Different strike price increments and ranges of strikes are considered here. Data are obtained for every trading day and the forecasts are based on re-estimating the parameters of the different regressions each day with a fixed length Rolling Window (RW) made up of the previous 1000 days. Ranking is obtained for different cases of strike increments and represents the average volatility forecasting performances of implied volatilities across different strike ranges.

TABLE 4 Simulation study with the use of interpolation-extrapolation method: out-of-sample forecast losses

	MSE		Ranking		Out-of-sample R^2 (%)		Ranking	
	Volatility	Log volatility	Volatility	Log volatility	Volatility	Log volatility	Volatility	Log volatility
VIX_{Theo}	0.0387	0.0190			74.5090	76.8332		
rv_{t-1}	0.0558	0.0287			63.2640	65.1061		
VIX	0.0568	0.0269	5	5	62.6171	67.2937	5	5
$MFIV$	0.0564	0.0266	4	4	62.8468	67.6101	4	4
$CXNT$	0.0519	0.0258	3	3	65.8194	68.6326	3	3
$CXLT$	0.0577	0.0280	6	6	62.0262	65.9059	6	6
$CXRT$	0.0504	0.0244	2	2	66.8396	70.3366	2	2
VC	0.0496	0.0231	1	1	67.3493	71.8709	1	1
VP	0.0662	0.0311	7	7	56.3911	62.1576	7	7
$CP-MFIV$	0.0525 (−0.39%)	0.0259 (−0.07%)	4	4	65.3974 (4.06%)	68.4538 (1.25%)	4	4
$CP-CXNT$	0.0522 (0.03%)	0.0259 (0.01%)	3	3	65.6338 (−0.28%)	68.4592 (−0.25%)	3	3
$CP-CXLT$	0.0563 (−0.14%)	0.0279 (−0.01%)	5	5	62.9527 (1.49%)	66.0735 (0.25%)	5	5
$CP-CXRT$	0.0480 (−0.24%)	0.0236 (−0.08%)	2	2	68.4057 (2.34%)	71.2650 (1.32%)	2	2
$CP-VC$	0.0444 (−0.52%)	0.0217 (−0.14%)	1	1	70.7738 (5.08%)	73.6136 (2.42%)	1	1
$CP-VP$	0.0605 (−0.58%)	0.0298 (−0.13%)	6	6	60.1917 (6.74%)	63.7520 (2.57%)	6	6

This table reports the ratio of the losses (MSE and R^2) for different predictive regressions for future monthly realized volatility and logarithm of volatility, respectively. For values of MSE, the numbers in parenthesis are the relative differences, squared forecasting errors, between the raw implied volatilities and those with the method of interpolation and extrapolation; values in bold represent significant differences at 5% level, indicated by the Diebold–Mariano test. For values of R^2 , the numbers in parenthesis are the percentage changes of the CP-measures with respect to the corresponding measures based on the observed options only; numbers in bold highlight the gains of the CP-measures. Ranking is obtained for cases where measures are constructed by observed options only and by prices with the use of interpolation and extrapolation, respectively.

TABLE 5 Simulation study: multi-period return prediction

			Return predictability (Adj R^2 %)		Ranking	
			30-day	60-day	30-day	60-day
VIX_{Theo}			0.7611	7.4725		
$\Delta K = 5$	N_K	Moneyness Range				
VIX	86	[0.8, 1.2]	1.4033	8.5224	4	4
	128	[0.7, 1.3]	1.2048	8.3069		
	167	[0.6, 1.4]	1.0217	8.0018		
MFIV	86	[0.8, 1.2]	1.4689	8.6001	2	3
	128	[0.7, 1.3]	1.2625	8.3965		
	167	[0.6, 1.4]	1.0648	8.0852		
CXNT	86	[0.8, 1.2]	0.7559	7.4092	7	7
	128	[0.7, 1.3]	0.7559	7.4092		
	167	[0.6, 1.4]	0.7559	7.4092		
CXLT	86	[0.8, 1.2]	1.1687	8.1426	5	5
	128	[0.7, 1.3]	1.0992	8.0754		
	167	[0.6, 1.4]	0.9731	7.8621		
CXRT	86	[0.8, 1.2]	1.0860	8.1113	6	6
	128	[0.7, 1.3]	0.9967	7.9809		
	167	[0.6, 1.4]	0.9164	7.8265		
VC	86	[0.8, 1.2]	1.6091	8.8549	1	1
	128	[0.7, 1.3]	1.3245	8.5471		
	167	[0.6, 1.4]	1.1319	8.2404		
VP	86	[0.8, 1.2]	1.4520	8.6069	3	2
	128	[0.7, 1.3]	1.2745	8.4381		
	167	[0.6, 1.4]	1.0611	8.1023		
$\Delta K = 1$						
VIX	422	[0.8, 1.2]	1.4875	8.6919	4	4
	629	[0.7, 1.3]	1.2448	8.3953		
	1239	[0.6, 1.4]	1.0541	8.0624		
MFIV	422	[0.8, 1.2]	1.5257	8.7259	2	2
	629	[0.7, 1.3]	1.2881	8.4596		
	1239	[0.6, 1.4]	1.0907	8.1320		
CXNT	422	[0.8, 1.2]	0.7798	7.4631	7	7
	629	[0.7, 1.3]	0.7798	7.4631		
	1239	[0.6, 1.4]	0.7798	7.4631		
CXLT	422	[0.8, 1.2]	1.2324	8.2971	5	5
	629	[0.7, 1.3]	1.1336	8.1630		
	1239	[0.6, 1.4]	1.0068	7.9322		
CXRT	422	[0.8, 1.2]	1.1023	8.1470	6	6
	629	[0.7, 1.3]	1.0128	8.0122		
	1239	[0.6, 1.4]	0.9320	7.8527		
VC	422	[0.8, 1.2]	1.4980	8.8190	3	1
	629	[0.7, 1.3]	1.2473	8.5171		
	1239	[0.6, 1.4]	1.0707	8.2103		

(Continues)

TABLE 5 (Continued)

			Return predictability (Adj R^2 %)		Ranking	
			30-day	60-day	30-day	60-day
VP	422	[0.8, 1.2]	1.5611	8.6914	1	3
	629	[0.7, 1.3]	1.3228	8.4411		
	1239	[0.6, 1.4]	1.1071	8.0958		

This table shows the adjusted R^2 from the daily regressions of the h -period returns on the current implied variance levels. Ranking is obtained for different cases of strike increments and represents the average ability of implied volatilities for predicting returns across different strike ranges.

deteriorate with the strike range. Second, with a finer partition of strikes, return predictive power generally improves, with the one exception of VC. From this evidence, only the interpolation method, which provides a smaller partition of strikes, is needed to achieve better return predictions by measures of implied volatility. Consistent with the work of Andersen, Fusari, and Todorov (2015), the deep OTM put options dominate the deep OTM call options in predicting future returns. This is indicated by the higher R^2 s given by the *CXLT* relative to those by the *CXRT*. In addition, the VC displays the strongest predictive power for future returns in most cases while the VP serves as the top performer only in the case of $\Delta K = 1$ when short horizon is considered. This suggests that OTM call options exhibit superior predictive power overall to that of the OTM put options for future returns. This is despite the superiority of the deep OTM puts over the deep OTM calls in this exercise.

Finally, the cubic spline is applied to achieve a finer partition of strikes in the case of return predictions. Measures of implied volatility based upon the options using the interpolation method are prefixed by C-. To examine the effect of the interpolation procedure on return predictions, this study takes the case of $\Delta K = 5$ and moneyness range = [0.8, 1.2] as an example and reports the results of the return predictability in Table 6. Gains in the predictive power for future returns are only observed for C-CXNT, C-CXLT, C-CXRT over 30- and 60-day horizons, and for C-VP over 30-day horizon. However, given the positive impact of the strike increment on return predictions in Table 5, the interpolation procedure is expected to lead to more evident gains in the predictive power of various implied volatilities for future returns, where the partition of strikes is often much more sparse, that is, greater than 5. Findings in section 6 confirm this hypothesis.

TABLE 6 Simulation study with the use of interpolation method: multi-period return prediction

	Return predictability (Adj R^2 %)		Ranking	
	30-day	60-day	30-day	60-day
VIX_{Theo}	0.7611	7.4725		
VIX	1.4033	8.5224	4	4
MFIV	1.4689	8.6001	2	2
CXNT	0.7559	7.4092	7	7
CXLT	1.1687	8.1426	5	5
CXRT	1.0860	8.1113	6	6
VC	1.6091	8.8549	1	1
VP	1.4520	8.6069	3	3
C-MFIV	1.4611 (−0.53%)	8.5874 (−0.15%)	3	2
C-CXNT	0.7799 (3.17%)	7.4629 (0.72%)	6	6
C-CXLT	1.1828 (1.21%)	8.1725 (0.37%)	4	4
C-CXRT	1.1016 (1.44%)	8.1354 (0.30%)	5	5
C-VC	1.4937 (−7.18%)	8.7952 (−0.67%)	1	1
C-VP	1.4639 (0.82%)	8.4910 (−1.35%)	2	3

This table shows the adjusted R^2 from the daily regressions of the h -period returns on the current implied variance levels. Numbers in parenthesis represent the percentage changes of the adjusted R^2 of the C-measures with respect to their corresponding measures based on observed options only. Numbers in bold highlight the gains in the return predictability by the C-measures. Ranking is obtained for cases where measures are constructed by observed options only and by prices with the use of interpolation, respectively.

TABLE 7 Empirical study: summary statistics

	Mean	SD	25%	50%	75%	Skewness	Kurtosis	ρ_1	ρ_{21}	ρ_{63}
<i>RV</i>	11.1303	7.2109	6.9544	8.8190	12.3023	3.1585	15.8942	0.9981	0.7671	0.4531
<i>RX</i>	17.2084	7.6473	12.1256	15.2086	19.5409	2.1455	9.1302	0.9810	0.8023	0.5563
<i>MFIV</i>	17.2422	7.6435	12.1511	15.2488	19.5459	2.15415	9.18317	0.9809	0.8020	0.5563
<i>CXNT</i>	11.4029	5.2737	7.9047	9.7784	13.2237	2.0799	8.8063	0.9793	0.8016	0.5570
<i>CXLT</i>	21.0587	8.8156	15.4129	18.7203	23.7711	2.1243	8.8417	0.9679	0.7485	0.5007
<i>CXRT</i>	17.3546	8.2176	11.4495	15.3165	20.3142	1.6119	5.8851	0.9620	0.7543	0.5743
<i>VC</i>	12.7696	6.2396	8.3591	11.0583	15.0483	1.6374	6.0523	0.9528	0.7396	0.5644
<i>VP</i>	18.3542	8.0187	13.3445	16.1713	20.4744	2.2383	9.5957	0.9626	0.7341	0.4847
<i>CP-MFIV</i>	16.5469	7.6433	11.3773	14.4459	19.1326	2.1054	8.9193	0.9810	0.8001	0.5558
<i>CP-CXNT</i>	11.0137	5.1739	7.5377	9.4473	12.8460	2.1251	9.0571	0.9813	0.8038	0.5581
<i>CP-CXLT</i>	15.3803	7.1542	10.5873	13.4761	17.8154	2.1162	9.0209	0.9810	0.7891	0.5524
<i>CP-CXRT</i>	12.5612	5.8506	8.6225	10.7398	14.5407	2.0982	8.8405	0.9808	0.8074	0.5631
<i>CP-VC</i>	9.4145	4.3973	6.4795	8.0340	10.9034	2.1150	8.9629	0.9777	0.8109	0.5699
<i>CP-VP</i>	13.5061	6.3572	9.2902	11.8622	15.5371	2.1608	9.3899	0.9797	0.7910	0.5434

This table reports summary statistics for various volatility measures. All the numbers are percentages. The data under analysis ranges from Jan 02, 2003 to Dec 31, 2013, with a total of 2330 observations. After aggregating realized volatility to monthly level, the number of observations reduces to 2307.

5 | DATA

The data sample spans from January 02, 2003 to December 31, 2013, encompassing 2769 trading days. Data are taken from several sources. Closing bid and ask SPX option prices and dividend yield are obtained from Optionmetrics via the WRDS system. High-frequency data at 5-min intervals for the SPX¹³ are collected from the Tick Data, Inc. Daily 1- and 3-month Treasury-bill yields,¹⁴ taken as the risk-free rates, are extracted from the Federal Reserve Bulletin. In addition, the average of bid and ask is taken as the best available measure of the option price to alleviate the bid-ask bounce problem. For the two nearby maturities, there is an average of 34 out of 97 (63 out of 97) OTM call (put) option quotes per day. Two commonly used data filters are applied. First, options with less than 7 days remaining to maturity are excluded. These options may be subject to problems of liquidity and market microstructure. Second, options violating the boundary conditions, that is, with BS implied volatilities below zero or above 100%, are excluded from the sample. Only OTM options are included since in-the-money options are less liquid and thus may induce bias into the computation of implied volatilities.

The CBOE calculates the *VIX* index using option prices updated every 5 min. However, the Optionmetrics database includes the last daily bid-ask quote only, which might not correspond to the data published by CBOE for their final end-of-day computation. Hence, as a more direct benchmark, this paper derives a replicated *VIX* index, *RX*, using the exact CBOE procedure every day. Thereby, it follows the work of Andersen, Bondarenko, and Gonzalez-Perez (2015). The *RX* provides an equivalent of the *VIX* using the SPX option prices from the Optionmetrics data set. It is well known that the CBOE adopts a particular rule to exclude OTM options: once two puts (calls) with consecutive strikes are found to have zero bid option prices, no puts (calls) with lower (higher) strikes are taken into account. The model-free implied volatility index with a broader strike range, denoted by *MFIV*, can be obtained by discarding any options with a zero bid price and employing all OTM options with a positive bid quote, that is, ignoring the cutoff rule by the CBOE. Hence, the *MFIV* provides an upper bound for *RX*. In addition, the same notations are adopted for the other candidate measures as those in the simulation study.¹⁵

¹³In order to measure the return variation during the overnight period, the squared overnight returns, computed as the squared close-to-open logarithmic price change, are added to the realized variance obtained over the trading day.

¹⁴Following the work of Jiang and Tian (2007), the risk-free rate is linearly interpolated between these two yields. However, when the maturity is shorter (longer) than 1 (3) month, the 1-month (3-month) yield is adopted.

¹⁵Throughout the empirical work, this paper makes use of the robust forward *F* as in the work of Andersen, Bondarenko, and Gonzalez-Perez (2015) rather than the “implied” forward *F* determined by the CBOE according to put-call parity. However, the CBOE *F* is still employed in computing the *RX* in order to approximate the *VIX*.

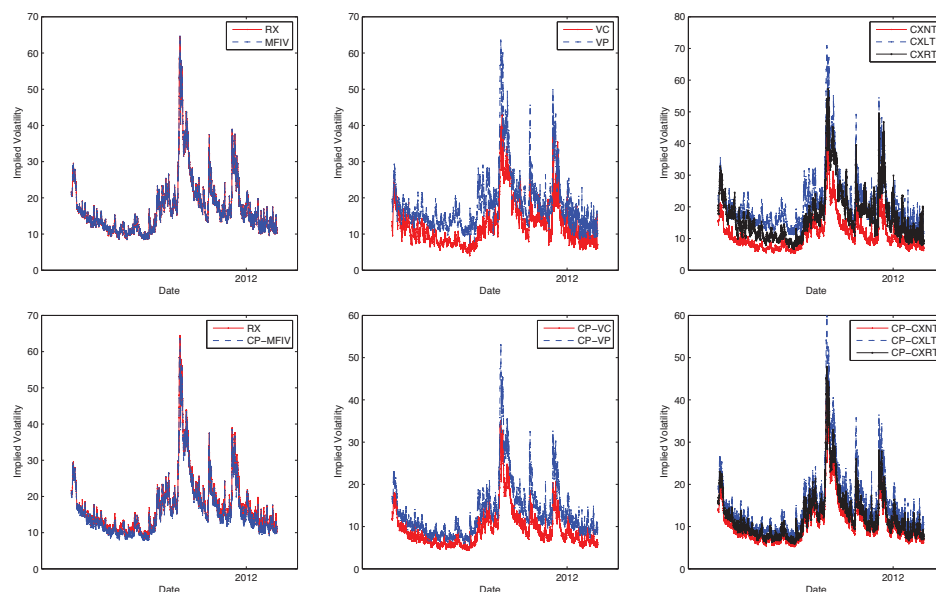


FIGURE 1 Time series plots. Data covers the period of Jan 02, 2003 to Dec 31, 2013 [Color figure can be viewed at wileyonlinelibrary.com]

For the 2769 trading days under consideration, the implied volatility measures are not available at some points due to a variety of reasons, including: (i) the requirement for the two nearby maturities is not satisfied; (ii) the lack of OTM options; and (iii) boundary conditions are violated, which reduces the sample size to 2330. The construction of the RV_t leads to the loss of 1 month at the end. Finally, the sample data under analysis contains 2307 observations, for the period from January 02, 2003 to November 27, 2013.

6 | EMPIRICAL RESULTS

This section starts by reporting the basic statistical properties of different volatility measures. It then investigates their performance as predictors of the future realized volatility and market returns of the underlying S&P 500 index.

Table 7 reports the summary statistics¹⁶ of the monthly volatility measures which are annualized and recorded daily. First, the unconditional mean of most implied volatility measures clearly exceeds the mean of the RV . This is consistent with the extant literature establishing the presence of a substantial positive risk premium for bearing volatility risk. Note also that the RV has the highest skewness and kurtosis statistics. This erratic nature is attributed to the unpredictable innovation term of the RV as noted in the work of Andersen and Bondarenko (2007). Second, the $CXLT$ (VP) is found to be more volatile and higher in magnitude than the $CXRT$ (VC) because deep OTM puts generally have the highest implied volatility, that is, volatility smile. A similar phenomenon is observed in the case of the CP -measures. Such evidence is also given in Figure 1 which depicts the time-variation of various implied volatility candidates. In particular, the RX overlaps the $MFIV$ closely and thus high similarity is expected in their forecasting power for future realized volatility and returns. Finally, all volatility measures exhibit substantial persistence with extremely slow decay in their autocorrelations.

The correlation between various measures of implied volatility and realized volatility is provided in Table 8. Compared with the measures extracted from the listed options only, the corresponding CP -measures display higher correlation with the RV . This is indicative of superior forecasting power for future volatility. Contrast to the work of Zhang et al. (2013) and Dotsis and Vlastakis (2016) who examine the information content¹⁷ of implied volatilities in in-sample regressions, this study concentrates on their OOS volatility forecasting performances. The results of the volatility forecasts are presented in Table 9 where the forecasting performance is measured by the MSE

¹⁶In the empirical study, the $MFIV$ is computed in the same way as the CBOE VIX in equation (4) but it ignores the cutoff rule by the CBOE. The VC and VP are computed as equations (2) and (3). This explains why $MFIV^2 \neq VC^2 + VP^2$ in Table 7. The reason for the use of the CBOE computation procedure, instead of the traditional $MFIV$ calculation method, is that the latter results in poorer forecasting performance compared with the RX . All the other measures are computed in the same way as in our simulation study. The results for the $MFIV$ constructed by equation (1) can be obtained from the author upon request.

¹⁷This paper also conducts in-sample regressions to examine the volatility forecasting ability of various measures of implied volatility. Results show that the interpolation and extrapolation procedure largely improves the explanatory power of the implied volatilities in all cases. For the sake of brevity, results are not reported but can be obtained from the author upon request.

TABLE 8 Correlation matrix

	<i>RV</i>	<i>RX</i>	<i>MFIV</i>	<i>CP-MFIV</i>	<i>CXNT</i>	<i>CP-CXNT</i>	<i>CXLT</i>	<i>CP-CXLT</i>	<i>CXRT</i>	<i>CP-CXRT</i>	<i>VC</i>	<i>CP-VC</i>	<i>VP</i>	<i>CP-VP</i>
<i>RV</i>	1.0000	0.7482	0.7487	0.7536	0.7585	0.7629	0.7389	0.7519	0.6500	0.7608	0.6299	0.7510	0.7248	0.7405
<i>RX</i>		1.0000	0.9999	0.9967	0.9895	0.9936	0.9714	0.9969	0.9290	0.9916	0.9041	0.9754	0.9488	0.9852
<i>MFIV</i>			1.0000	0.9967	0.9893	0.9936	0.9726	0.9968	0.9301	0.9916	0.9050	0.9754	0.9500	0.9850
<i>CP-MFIV</i>				1.0000	0.9937	0.9974	0.9677	0.9995	0.9206	0.9962	0.8968	0.9799	0.9451	0.9861
<i>CXNT</i>					1.0000	0.9973	0.9581	0.9915	0.9126	0.9972	0.8896	0.9844	0.9325	0.9773
<i>CP-CXNT</i>						1.0000	0.9657	0.9959	0.9154	0.9991	0.8930	0.9848	0.9419	0.9821
<i>CXLT</i>							1.0000	0.9682	0.9224	0.9628	0.8939	0.9422	0.9718	0.9539
<i>CP-CXLT</i>								1.0000	0.9191	0.9934	0.8947	0.9756	0.9467	0.9872
<i>CXRT</i>									1.0000	0.9169	0.9623	0.9050	0.8955	0.9075
<i>CP-CXRT</i>										1.0000	0.8951	0.9875	0.9377	0.9790
<i>VC</i>											1.0000	0.9008	0.9022	0.9017
<i>CP-VC</i>												1.0000	0.9397	0.9812
<i>VP</i>													1.0000	0.9618
<i>CP-VP</i>														1.0000

The sample period is from Jan 02, 2003 to 27 Nov, 2013, with a total of 2307 observations.

TABLE 9 Empirical study: out-of-sample forecast losses

	MSE		Ranking		Out-of-sample R^2 (%)		Ranking	
	Volatility	Log volatility	Volatility	Log volatility	Volatility	Log volatility	Volatility	Log volatility
$N_C = 34, N_P = 63$				$N_C = 34, N_P = 63$				
rv_{t-1}	0.1943	0.1930			37.5615	29.6396		
RX	0.1556	0.1393	3	3	50.0027	49.2033	3	3
$MFIV$	0.1554	0.1390	2	2	50.0604	49.3357	2	2
$CXNT$	0.1552	0.1306	1	1	50.1026	52.3644	1	1
$CXLT$	0.1802	0.1485	4	4	42.0750	45.8654	4	4
$CXRT$	0.2315	0.1971	6	6	25.6019	28.1317	6	6
VC	0.2463	0.2114	7	7	20.8354	22.9354	7	7
VP	0.1831	0.1540	5	5	41.1424	43.8649	5	5
$N_C = 308, N_P = 308$				$N_C = 308, N_P = 308$				
$CP-MFIV$	0.1545 (−0.09%)	0.1358 (−0.32%)	3	4	50.3542 (0.59%)	50.5030 (2.37%)	3	4
$CP-CXNT$	0.1502 (−0.50%)	0.1288 (−0.18%)	1	1	51.7218 (3.23%)	53.0330 (1.28%)	1	1
$CP-CXLT$	0.1549 (−2.53%)	0.1378 (−1.07%)	4	5	50.2225 (19.36%)	49.7529 (8.48%)	4	5
$CP-CXRT$	0.1524 (−7.90%)	0.1297 (−6.74%)	2	2	51.0072 (99.23%)	52.7195 (87.40%)	2	2
$CP-VC$	0.1557 (−9.06%)	0.1309 (−8.05%)	5	3	49.9474 (139.72%)	52.2884 (127.98%)	5	3
$CP-VP$	0.1576 (−2.56%)	0.1419 (−1.21%)	6	6	49.3625 (19.98%)	48.2794 (10.06%)	6	6

This table reports the ratio of the losses (MSE and R^2) for different predictive regressions for future monthly realized volatility and logarithm of volatility, respectively. Data are obtained for every trading day and the forecasts are based on re-estimating the parameters of the different regressions each day with a fixed length Rolling Window (RW) made up of the previous 1000 days. For values of MSE, the numbers in parenthesis are the relative differences, squared forecasting errors, between the raw implied volatilities and those with the method of interpolation and extrapolation; values in bold represent significant differences at 5% level, indicated by the Diebold–Mariano test. For values of R^2 , the numbers in parenthesis are the percentage changes of the CP-measures with respect to the corresponding measures based on the observed options only; numbers in bold highlight the gains of the CP-measures. Ranking is obtained for cases where measures are constructed by observed options only and by prices with the use of interpolation and extrapolation, respectively. N_C denotes the number of OTM call options involved and N_P stands for the number of OTM put options.

and OOS R^2 . Gains achieved by the CP-measures are generally more evident than those in the simulation study. In almost all cases, gains in MSE are significant at 5% level. The CXNT dominates other measures that are based on the existing options. The CP-CXNT ranks best among all CP-measures. As shown in the upper panel of Table 9, CXLT (VP) outperforms the CXRT (VC) in the forecasting of future volatility. This can be attributed to the fact that only a very small number of OTM calls (34 out of 97 per day on average) are available in this empirical study. However, in the lower panel, where more options are involved with the use of interpolation and extrapolation scheme, the OTM call options are superior to the OTM puts, indicated by the better forecasting performance of the CP-CXRT (CP-VC) than that of the CP-CXLT (CP-VP). The evidence for the advantage of the OTM calls is in line with the simulation result discussed in section 4. Moreover, conclusions drawn from Table 9 remain intact when different loss functions for OOS forecasts are considered.

Finally, the return predictability is evaluated by various implied volatilities using equation (18) where the excess returns are considered as opposed to raw returns. To better understand the predictive power of implied volatilities for future returns in different market conditions, this study further splits the data sample into pre-crisis and post-crisis periods. The beginning of the financial crisis is set at September 01, 2007. As discussed in the simulation study, only interpolation is needed in the exercise of return predictions. Values of the adjusted R^2 implied by different return regressions are reported in Table 10. In the pre-crisis period, the interpolation improves the return predictive power for 4 out of 12 measures. In the post-crisis period, this result holds for 7 out of 12 measures. Moreover, the C-VC dominates all the other implied volatilities in terms of the performance for predicting future returns in the post-crisis period. The CXRT performs the best in such forecasting practice in the pre-crisis period. Hence, the results suggest a few good substitutes for the VIX index as predictors for future returns. In the upper panel of

TABLE 10 Empirical study: multi-period return prediction

	Return predictability (Adj R^2 %)				Ranking			
	Pre-crisis		Post-crisis		Pre-crisis		Post-crisis	
	$N_C = 19, N_P = 35$		$N_C = 35, N_P = 82$					
	30-day	60-day	30-day	60-day	30-day	60-day	30-day	60-day
<i>RX</i>	8.2435	8.5540	10.7008	17.2237	5	5	3	3
<i>MFIV</i>	8.3097	8.5988	10.7418	17.2416	4	4	2	2
<i>CXNT</i>	9.1953	9.7213	12.5409	19.1597	3	3	1	1
<i>CXLT</i>	6.0534	5.5339	9.8895	15.4502	6	6	4	4
<i>CXRT</i>	10.5308	15.1420	4.5173	12.7485	1	1	7	7
<i>VC</i>	10.2042	14.3142	4.7760	12.5935	2	2	6	6
<i>VP</i>	3.7819	2.8295	8.9308	14.0298	7	7	5	5
	$N_C = 136, N_P = 371$		$N_C = 397, N_P = 216$					
<i>C-MFIV</i>	8.0393 (−3.25%)	7.9514 (−7.53%)	10.5657 (−1.64%)	16.8208 (−2.44%)	3	3	4	4
<i>C-CXNT</i>	7.8481 (−14.65%)	7.8074 (−19.69%)	13.0164 (3.79%)	19.0621 (−0.51%)	4	4	3	3
<i>C-CXLT</i>	7.3816 (21.94%)	6.9832 (26.19%)	9.7139 (−1.78%)	16.0005 (3.56%)	5	5	5	5
<i>C-CXRT</i>	8.7838 (−16.59%)	9.2190 (−39.12%)	13.8248 (206.04%)	19.7243 (54.72%)	2	2	2	2
<i>C-VC</i>	9.7937 (−4.02%)	10.8748 (−24.03%)	15.0924 (216.01%)	20.7174 (64.51%)	1	1	1	1
<i>C-VP</i>	6.8616 (81.43%)	6.2286 (120.14%)	8.4636 (−5.23%)	14.7009 (4.78%)	6	6	6	6

This table shows the adjusted R^2 from the daily regressions of the h -period returns on the current implied variance levels. Numbers in parenthesis represent the percentage changes of the adjusted R^2 of the C -measures with respect to their corresponding measures based on observed options only. Numbers in bold highlight the gains in the return predictability by the C -measures. Ranking is obtained for cases where measures are constructed by observed options only and by prices with the use of interpolation, respectively. N_C denotes the number of OTM call options involved and N_P stands for the number of OTM put options.

Table 10, where measures are derived from the observed option prices only, the OTM call options exhibit greater predictive power for future returns than the OTM put options in the pre-crisis period while the OTM put options play a more dominant role in the post-crisis period. In the lower panel, where the cubic spline is used to interpolate between available strikes, OTM call options outperform OTM put option in predicting future returns in both pre- and post-crisis periods. This is consistent with the evidence found in the simulation study.

7 | CONCLUSION

This paper examines the forecasting power of various model-free option-implied volatilities for future returns and realized volatility via both Monte Carlo simulations and an empirical study using SPX options. By decomposing the model-free implied volatility into different components using various segments of the out-of-the money (OTM) put and call options, this study ascertains the role of each of the components. The paper provides a simulation study on the impact of the strike range and increment on the predictive power of the implied volatilities. Results show that: first, the forecast accuracy for future volatility improves with the range of strikes; second, the strike range exerts a negative impact on the predictive power of the implied volatilities for future returns; third, a smaller partition of strikes tends to result in greater performance of implied volatilities in predicting returns. These findings warrant the application of an interpolation and extrapolation scheme in order to enhance the forecasting power of implied volatilities for future volatility while only an interpolation method is needed in the case of return predictions.


In both simulation and empirical studies, the superiority of the aforementioned technique, that is, interpolation/extrapolation methods, is observed for most measures considered in forecasts of future returns and volatility. More interestingly, once this technique is implemented in the empirical case to overcome the problem of the lack of strikes, the OTM SPX call options clearly exhibit higher forecasting power than the OTM put options. This accords with the evidence from the simulation experiment. On the other hand, the advantages of the OTM SPX put options are noted when implied volatilities are derived from the listed options only.

ACKNOWLEDGMENTS

Xingzhi Yao gratefully acknowledges the financial support from the Economic and Social Research Council [grant number: ES/J500094/1]. The authors thank the participants at the 10th International Conference on Computational and Financial

Econometrics (Seville 2016) and the 15th INFINITI Conference on International Finance (Valencia 2017). The authors are grateful to Torben Andersen, Eduardo Rossi, and an anonymous referee for insightful comments, which help to improve the paper. The paper has benefited from the codes shared by Jin-Chuan Duan, Chung-Ying Yeh, and Oleg Bondarenko. The authors are also thankful to Gerry Steele for helpful editorial suggestions.

ORCID

Xingzhi Yao  <http://orcid.org/0000-0001-9633-5494>

REFERENCES

- Andersen, T., Bollerslev, T., & Diebold, F. (2007). Roughing it up: Including jump components in the measurement, modeling, and forecasting of return volatility. *The Review of Economics and Statistics*, 89(701), 720.
- Andersen, T. G., & Bondarenko, O. (2007). Construction and interpretation of model-free implied volatility. In I. Nelken (Ed.), *Volatility as an asset class* (pp. 141–181). London, UK: Risk Books.
- Andersen, T. G., Bondarenko, O., & Gonzalez-Perez, M. T. (2015). Exploring return dynamics via corridor implied volatility. *The Review of Financial Studies*, 28, 2902–2945.
- Andersen, T. G., Fusari, N., & Todorov, V. (2015). The risk premia embedded in index options. *Journal of Financial Economics*, 117, 558–584.
- Ang, A., Hodrick, R. J., Xing, Y., & Zhang, X. (2006). The cross-section of volatility and expected returns. *Journal of Finance*, 61, 259–299.
- Banerjee, P. S., Doran, J. S., & Peterson, D. R. (2007). Implied volatility and future portfolio returns. *Journal of Banking and Finance*, 31, 3183–3199.
- Barndorff-Nielsen, O. E., & Shephard, N. (2002). Econometric analysis of realized volatility and its use in estimating stochastic volatility models. *Journal of the Royal Statistical Society. Series B: Statistical Methodology*, 64, 253–280.
- Bates, D. S. (2008). The market for crash risk. *Journal of Economic Dynamics and Control*, 32, 2291–2321.
- Bates, D. S. (2012). U.S. stock market crash risk, 1926–2010. *Journal of Financial Economics*, 105, 229–259.
- Bondarenko, O. (2003). Estimation of risk-neutral densities using positive convolution approximation. *Journal of Econometrics*, 116, 85–112.
- Britten-Jones, M., & Neuberger, A. (2000). Option prices, implied price processes, and stochastic volatility. *Journal of Finance*, 55, 839–866.
- Carr, P., & Wu, L. (2006). A tale of two indices. *The Journal of Derivatives*, 13, 13–29.
- Cox, J. C., Ingersoll, J. E., & Ross, S. A. (1985). A theory of the term structure of interest rates. *Econometrica*, 53, 385–407.
- Demeterfi, K., Derman, E., Kamal, M., & Zou, J. (1999). More than you ever wanted to know about volatility swaps. Working Paper, Goldman Sachs.
- Dotsis, G., & Vlastakis, N. (2016). Corridor volatility risk and expected returns. *Journal of Futures Markets*, 36, 488–505.
- Duan, J.-C., & Simonato, J.-G. (1998). Empirical martingale simulation for asset prices. *Management Science*, 44, 1218–1233.
- Duan, J.-C., & Yeh, C.-Y. (2010). Jump and volatility risk premiums implied by VIX. *Journal of Economic Dynamics and Control*, 34, 2232–2244.
- Giot, P. (2005). Relationships between implied volatility indexes and stock index returns. *The Journal of Portfolio Management*, 31, 92–100.
- Guo, H., & Whitelaw, R. F. (2006). Uncovering the risk-return relation in the stock market. *The Journal of Finance*, 61, 1433–1463.
- Hilal, S., Poon, S.-H., & Tawn, J. (2011). Hedging the black swan: Conditional heteroskedasticity and tail dependence in S&P 500 and VIX. *Journal of Banking and Finance*, 35, 2374–2387.
- Jackwerth, J. C. (2000). Recovering risk aversion from option prices and realized returns. *The Review of Financial Studies*, 13, 433–451.
- Jiang, G. J., & Tian, Y. S. (2005). The model-free implied volatility and its information content. *The Review of Financial Studies*, 18, 1305–1342.
- Jiang, G. J., & Tian, Y. S. (2007). Extracting model-free volatility from option prices: An examination of the VIX index. *Journal of Derivatives*, 14, 35–60.
- Jones, C. S. (2006). A nonlinear factor analysis of S&P 500 index option returns. *The Journal of Finance*, 61, 2325–2363.
- Patton, A. J. (2011). Volatility forecast comparison using imperfect volatility proxies. *Journal of Econometrics*, 160, 246–256.
- Poon, S.-H., & Granger, C. (2003). Forecasting volatility in financial markets: A review. *Journal of Economic Literature*, 41, 478–539.
- Rossi, A., & Timmermann, A. (2010). What is the shape of the risk-return relation? Working Paper, University of California, San Diego.
- Taylor, S. J., Yadav, P. K., & Zhang, Y. (2010). The information content of implied volatilities and model-free volatility expectations: Evidence from options written on individual stocks. *Journal of Banking and Finance*, 34, 871–881.
- Zhang, Y., Taylor, S. J., & Wang, L. (2013). Investigating the information content of the model-free volatility expectation by monte carlo methods. *Journal of Futures Markets*, 33, 1071–1095.

How to cite this article: Yao X, Izzeldin M. Forecasting using alternative measures of model-free option-implied volatility. *J Futures Markets*. 2018;38:199–218. <https://doi.org/10.1002/fut.21881>